

URSI GASS 2020, Rome, Italy, 29 August - 5 September 2020



Air-filled Substrate-Integrated Waveguide Technology for Broadband and Highly-Efficient Photonic-Enabled Antenna Systems

Sam Lemey^{*(1)}, Olivier Caytan⁽¹⁾, Quinten Van den Brande⁽¹⁾, Igor Lima de Paula⁽¹⁾, Laurens Bogaert⁽¹⁾⁽²⁾, Haolin Li⁽¹⁾, Joris Van Kerrebrouck⁽¹⁾, Ad C. F. Reniers⁽³⁾, Bart Smolders⁽³⁾, Johan Bauwelinck⁽¹⁾, Piet Demeester⁽¹⁾, Guy Torfs⁽¹⁾, Dries Vande Ginste⁽¹⁾, Steven Verstuyft⁽²⁾, Bart Kuyken⁽²⁾, and Hendrik Rogier⁽¹⁾

(1) IDLab, Department of Information Technology, Ghent University-imec, 9052 Ghent, Belgium

(2) Photonics Research Group, Department of Information Technology, Ghent University-imec, 9052 Ghent, Belgium

(3) Department of Electrical Engineering, Eindhoven University of Technology, Eindhoven 5600, The Netherlands

Abstract

The combination of microwave photonics, radio-over-fiber (RoF) and air-filled substrate-integrated-waveguide (AFSIW) technology opens many promising pathways to realize robust, broadband, and highly-integrated multi-antenna systems that address the stringent demands of (beyond-)5G wireless applications. In this paper, we demonstrate the potential of such a multi-disciplinary approach by discussing three designs. First, two AFSIW-based photonic-enabled remote antenna units (RAUs) are presented for downlink sub-6 GHz RoF. By adopting an extensive full-wave/circuit co-simulation model, the power transfer between the optical and electrical domain is maximized. In the first design, this is done by using a Chebyshev impedance matching network, while the second design exploits conjugate matching. Second, a hybrid integration strategy for compact, broadband and highly efficient mmWave antennas is introduced. Its excellent performance is proven by realizing an on-chip AFSIW stacked patch antenna. In addition, the design facilitates compact integration of the opto-electronic front-end, making it attractive for the realization of next-generation photonic-enabled mmWave planar multi-antenna systems.

1 Introduction

5G standards are under heavy development and the first commercial 5G deployments are hitting the market, promising unrivaled performance in terms of data rate, latency and capacity [1]. Meanwhile, it has become clear that (large-scale) multi-antenna systems will play a major role in both 5G and beyond-5G wireless systems to satisfy the ever-increasing hunger towards higher data rates by exploiting (massive) multiple-in multiple-out (MIMO) techniques. In combination with larger bandwidth operation at sub-6 GHz and mmWave frequencies, these advanced antenna systems bring along a myriad of challenges to efficiently distribute broadband signals to a massive number of antennas. Microwave photonics, using ultra-wideband photonic components to process RF signals, and radio-over-fiber (RoF) architectures show great potential to alleviate these challenges. RoF exploits the advantages of optical fiber to effi-

ciently exchange radio signals between a central unit (CU) and multiple remote antenna units (RAUs). By centralizing most hardware at the CU, cost and complexity of the RAUs can be significantly reduced. This is especially pronounced for analog RoF and Sigma-Delta-over-Fiber schemes [2]. In both schemes, RAUs only need to implement conversion between the optical and electrical domain, while tight synchronization amongst the RAUs is guaranteed. Although this approach provides a powerful solution for the realization of scalable multi-antenna systems by co-locating or distributing an arbitrary number of RAUs, major research efforts are required (1) to realize compact, broadband and highly-efficient antennas, (2) to maximize power transfer between the optical and electrical domain, and (3) to maintain performance in realistic environments.

In this paper, we will discuss how these challenges may be tackled by using air-filled substrate-integrated-waveguide (AFSIW) antennas and adopting a system-oriented electronic-photonic co-optimization procedure. Thereto, two passive sub-6 GHz photonic-enabled AFSIW-based RAUs will be described. The first design maximizes power transfer from photodiode to antenna by using a distributed impedance matching network (IMN) [3]. The second design maximizes power transfer by conjugate matching of the antenna [4], thereby omitting the area-consuming IMN and its corresponding losses. In addition, we will discuss the challenges related to photonic-enabled mmWave RAUs and how these can be tackled by relying on AFSIW on-chip antennas [5].

2 AFSIW as Enabling Technology

The AFSIW technology has become well-established in microwave and mmWave applications because of its ability to realize robust and high-performance components in low-cost substrates (eg. FR4, PLA and silicon) at a low fabrication cost by relying on either standard PCB, 3-D-printing or silicon process technology [3, 4, 5]. As in this technology the electromagnetic (EM) fields are confined to air-filled metallized cavities, multiple strategic advantages arise for AFSIW-based photonic-enabled antenna systems.

First, dielectric losses are eliminated, leading to excellent radiation efficiencies. Second, mutual coupling in compact arrays can be minimized by suppressing surface waves. Third, a very high antenna-to-integration platform isolation can be obtained, which is essential to guarantee robust performance of the RAUs when deployed in realistic environments. In addition, the multi-layer stackup facilitates compact integration of the (opto-)electronic front-end hardware.

3 Fully-Passive Photonic-Enabled Remote Antenna Units for Sub-6-GHz RoF

Both presented sub-6 GHz RAUs [3, 4] (Fig. 1) consist of one antenna and focus on the downlink subsystem, which implements the wireless transmission of RF signals by the RAU. They are tailored towards the novel converged fiber/wireless system proposed in [6]. This system aims to provide high bandwidth, low latency and reliable wireless connectivity to a massive number of autonomous robots roaming through a futuristic factory. To support the high bit-rate density, the factory is subdivided in a large number of small attocells, which are served by floor-integrated photonic-enabled RAUs. The availability of compact, cost-effective and power-efficient RAUs is therefore vital to make this concept technically and economically viable. Thereto, both RAUs respect several strict design constraints. First of all, a passive conversion from the optical to the electric domain is enforced, hereby excluding all active components (e.g. electrical amplifiers) except for the photodiode. Under this constraint, the RF power radiated by the RAU originates entirely from the high-frequency current generated by the photodiode in response to its illumination. Therefore, it can be optimized by ensuring impedance matching between the photodiode and the antenna, so that the RF power transfer towards the antenna is maximized within the frequency band of interest. This results in a highly energy-efficient downlink RAU, whose transmit power and useful range are only limited by nonlinear distortion. In order to further enhance the units' cost-effectiveness and energy efficiency, low-profile and highly efficient antennas based on AFSIW technology are employed, which can be produced using standard PCB technology. Despite extensive specialization for their intended application [6], the proposed sub-6 GHz RAUs are extendable towards more conventional 5G applications, as discussed in the following subsections.

3.1 Design I: AFSIW Downlink RAU with a Chebyshev Matching Network

The first RAU relies on a nearly lossless lumped/distributed IMN to transform the $50\ \Omega$ AFSIW antenna impedance to match the photodiode's output impedance (Figs. 1a and b) [3]. This maximizes the radiated RF power in the frequency band of interest (3.3 GHz to 3.7 GHz) without electrical amplification. In addition, the photodiode is biased with 0 V leading to a fully-passive unit fed by a single multi-mode fiber. The IMN, photodiode, bias tee and multi-mode

fiber pigtail are integrated on the opto-electric (O/E) conversion PCB (Fig. 1a), which is implemented on a $508\ \mu\text{m}$ Rogers 4350B high-frequency laminate and employs one of both copper layers as a ground plane. As shown in the exploded view in Fig. 1a, this O/E PCB forms the backside of the AFSIW antenna, resulting in a low-profile and compact RAU. Two central 1.55 mm FR-4 cavity PCBs contain a rectangular air-filled region, which is created by milling and subsequent metallization of the inner edges. The air-filled region contains the antenna cavity's fields, hereby maximizing radiation efficiency. It is covered by the slot PCB, implemented on a $508\ \mu\text{m}$ Rogers 4350B substrate. Its inner metallic layer contains the antenna's radiating rectangular slot. The slot also divides the cavity into two coupled half-mode cavities. This gives rise to two distinct cavity resonances, which, in combination with the air substrate, yield an ultra-wide bandwidth ($\geq 10\ \text{dB}$ return loss from 3.1 GHz to 3.9 GHz). The circuitry on the O/E PCB excites the $50\ \Omega$ AFSIW antenna by means of a capacitively coupled probe feed. Fig. 1b explains the operating principle of the IMN. As discussed in [3], the IMN design procedure starts with an accurate characterization of the photodiode's output impedance, which is modelled at zero-bias by a $135.6\ \text{fF}$ junction capacitance in parallel with a photocurrent source i_p , and a $22.1\ \Omega$ series resistance. For such a generator, a third-order bandpass Chebyshev IMN is synthesized, which maximizes the minimum transducer gain in the 3.3 GHz–3.7 GHz frequency band, considering the $50\ \Omega$ antenna impedance as the load. Since $50\ \Omega$ is a common reference impedance, a power amplifier can be inserted directly in front of the antenna to enhance the transmit power and useful range when targeting more conventional 5G scenarios. After several transformations, the lumped/distributed circuit in Fig. 1b is obtained [3]. In the microwave implementation (Fig. 1a), the $15.3\ \text{nH}$ inductance is realized by a $7.2\ \text{nH}$ chip inductor, a tunable inductor based on a grounded coplanar waveguide stub and the photodiode's bondwires. Finally, the two half-wavelength open shunt stubs are realized by radial stubs. By means of an extensive full-wave/circuit cosimulation model of the RAU, the power transfer from photodiode to antenna is maximized, realizing an average transducer gain of 60.9% in the targeted frequency band. Additional simulated and measured performance metrics are given in Table 1, including the boresight gain (normalized w.r.t. the optical source's slope efficiency (SE) as in [4] (Fig. 1b)), the gain bandwidth, and the half-power beam width (HPBW).

3.2 Design II: Compact AFSIW Downlink RAU through Conjugate Matching

Although previous RAU is highly integrated, the distributed IMN consumes valuable space. In [4], a more thorough co-design of the IMN and antenna is conducted that eliminates the large distributed IMN, including its losses and spurious radiation, while also resulting in a more compact antenna topology. Nevertheless, as shown in Figs. 1c and d, both the RAU's structure and design procedure are very simi-

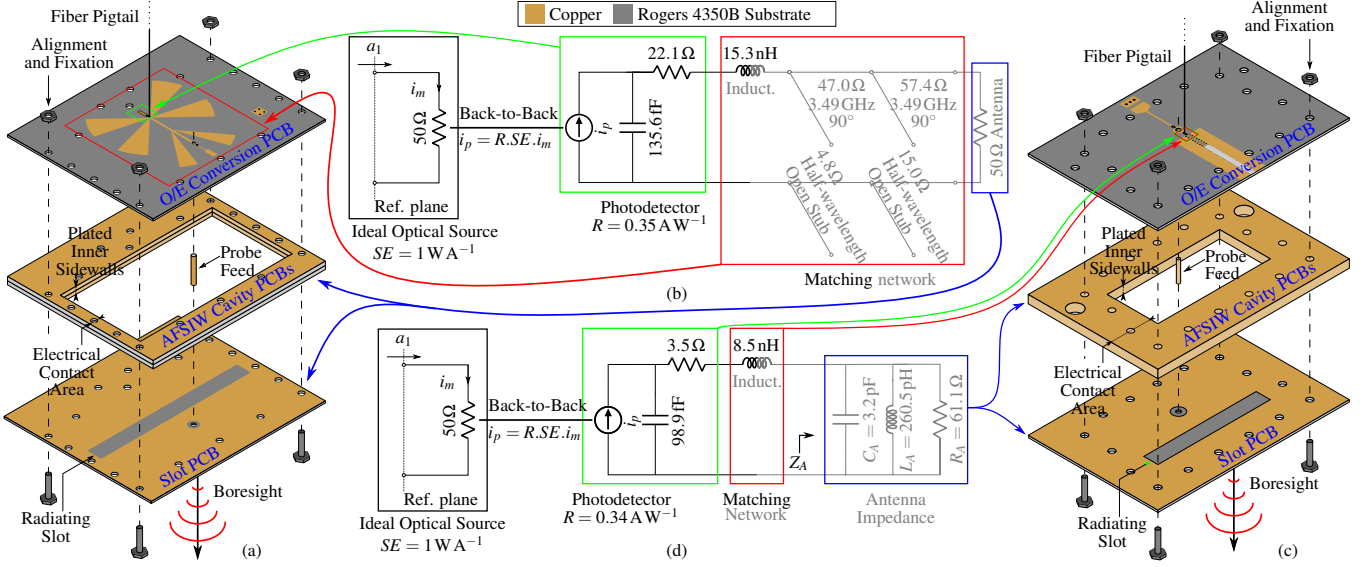


Figure 1. Passive downlink remote antenna unit (RAU) with lumped/distributed matching network (Design I) [3]: (a) exploded view and (b) circuit model. Similar figures (c) and (d) for the conjugate-matched design (Design II) [4].

lar. The design starts with the synthesis of a second order Chebyshev IMN based on an accurate characterization of the photodiode's impedance ($98.9 \text{ fF} + 3.5 \Omega$). An operating bandwidth ranging from 5.15 GHz to 5.85 GHz is targeted. Instead of realizing the resonant shunt LC tank as an area-consuming distributed element and transforming the antenna's 50Ω impedance to the required 61.1Ω by means of a quarter-wave transformer, as in Design I, the antenna element itself is now designed to exhibit the required frequency-dependent input impedance Z_A of the shunt RLC tank ($R_A || L_A || C_A$). This means that the antenna needs to exhibit a very low quality factor of only 6.8, which is possible by using an air-filled cavity. Whereas a coupled pair of half-mode AFSIW cavities was necessary to realize wideband impedance matching to 50Ω in Design I, a single half-mode AFSIW cavity suffices to realize the required input impedance Z_A . As a result, the distributed part of the IMN is eliminated and only the 8.5 nH inductance remains, which is realized similarly as in Design I. After extensive optimization, the full-wave/circuit cosimulation model predicts an average transducer gain of 19.2% in the considered frequency band. Comparison with Design I requires to account for the different photodiode impedance. Additional simulated and measured performance metrics are provided in Table 1. Both RAUs exhibit similar performance, while Design II is considerably more compact. In addition, it provides more space to also incorporate the uplink O/E conversion circuit. As such, it is an important step towards compact bi-directional (multi-antenna) RAUs.

4 Towards Broadband and Highly-Efficient mmWave Photonic-Enabled RAUs

When moving towards mmWave frequencies, multi-antenna RAUs with adaptive beamforming become indispensable to overcome the more challenging propagation

characteristics. Thereto, the antenna footprint should be reduced further below $0.5\lambda \times 0.5\lambda$ to support grating-lobe-free beamsteering when incorporated into a planar array. Due to the more prominent parasitic interconnect effects at mmWave frequencies, compact integration of antenna system and (opto-electronic) front-end hardware becomes increasingly important, urging the need for an antenna-on-chip (AoC) or antenna-in-package (AiP) solution. However, the former typically suffers from poor antenna performance due to the unfavorable properties of silicon, while the latter suffers from increased interconnect losses. To alleviate these issues, a novel hybrid on-chip integration strategy is proposed in [5] and illustrated in Fig. 2. An AFSIW cavity-backed stacked patch antenna is realized on a $600 \mu\text{m}$ -thick silicon substrate by relying on standard silicon fabrication processes, making it low cost and suitable for mass production. As depicted in Fig. 2, both the antenna feed and a metallized air-filled cavity are implemented on chip, whereas the stacked patch configuration is implemented on a high-frequency PCB laminate supporting the chip. This hybrid strategy allows compact integration of the (opto-electronic) front-end module at the back of the antenna element, thereby mitigating any interconnect losses, while simultaneously increasing the radiation efficiency up to 93% by keeping the EM-fields out of the lossy silicon. Furthermore, implementing the stacked-patch configuration allows to achieve a large bandwidth, while keeping the footprint below $0.5\lambda \times 0.5\lambda$. As a result, excellent antenna performance is obtained with respect to the state-of-the-art, when considering the combination of bandwidth, efficiency and antenna footprint as depicted in Table 2. As the hybrid on-chip antenna strategy shows great potential, the next step will consist of interfacing the antenna to an opto-electric front-end module by applying similar techniques as in Section 3. Thorough co-design between the antenna and the opto-electric interface (and ad-

Table 1. Measured (simulated) performance of the sub-6 GHz passive remote antenna units (RAUs) (f_c = center frequency).

	Footprint (A) [$\lambda \times \lambda$]	-3 dB Gain Bandwidth [GHz]	Boresight gain at f_c^* [dBi] (*normalized w.r.t. SE as in [4])	E/H-Plane HPBW at f_c [°]
Design I	1.19×0.66	3.27–3.75 (3.25–3.74)	10.8 (10.2)	150/55 (105/56)
Design II	0.84×0.41	4.98–6.00 (5.07–5.91)	10.5 (10.3)	117/62 (102/68)

Table 2. Our work (**bold**) compared to the state-of-the-art.

	f [GHz]	BW [%]	η [%]	A [$\lambda \times \lambda$]
[7]	60.0	11.80	90.0	0.61×0.95
[8]	34.5	4.00	95.0	1.15×1.15
[9]	68.0	5.70	96.7	0.16×0.28
[5]	28.5	13.00	90.9	0.49×0.49

ditional active electronics), will lead to a compact, highly efficient and profoundly integrated unit antenna element. Next, a planar remote opto-electronic antenna array unit, co-integrated with a photonic integrated true-time-delay-based beamforming network will be developed to demonstrate flexible high data-rate wireless connections for next-generation wireless applications.

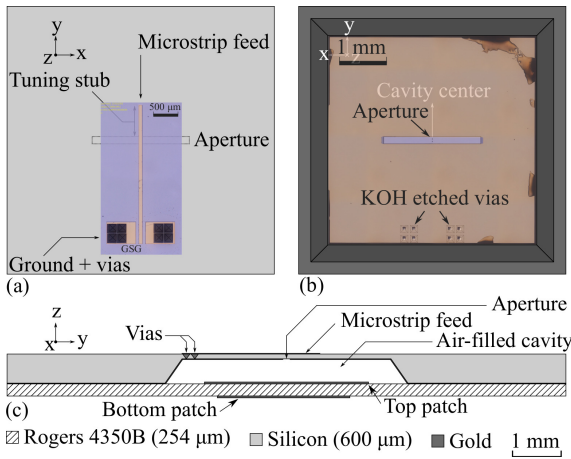


Figure 2. Hybrid on-chip antenna: (a) top view, (b) bottom view, and (c) cross-sectional view. Dimensions in [5].

5 Conclusion

In this contribution, we have discussed three designs to demonstrate the merits and potential of AFSIW technology and a system-oriented electronic-photonic co-optimization procedure to realize broadband, robust and high-performance photonic-enabled antenna systems. Measurements have been performed and demonstrate excellent performance, proving the potential of our multi-disciplinary approach. This may be a first step towards the realization of highly versatile large-scale sub-6 GHz and mmWave photonic-enabled multi-antenna systems, by distributing or co-locating an adequate amount of remote antenna units.

6 Acknowledgements

This work was supported in part by the ERC Advanced Grant ATTO project (No.695495).

References

- [1] A. Gupta and R. Jha, “A Survey of 5G Network: Architecture and Emerging Technologies,” *IEEE Access*, vol. 3, pp. 1206–1232, 2015.
- [2] L. Breyne, G. Torfs, X. Yin, P. Demeester, and J. Bauwelinck, “Comparison between Analog Radio-over-Fiber and Sigma Delta Modulated Radio-over-Fiber,” *IEEE Photonic Tech. L.*, vol. 29, no. 21, pp. 1808–1811, 2017.
- [3] O. Caytan, L. Bogaert, H. Li, J. Van Kerrebrouck, S. Lemey, G. Torfs, J. Bauwelinck, P. Demeester, S. Agneessens, D. Vande Ginste, and H. Rogier, “Passive Opto-Antenna as Downlink Remote Antenna Unit for Radio Frequency over Fiber,” *J. Light. Technol.*, vol. 36, no. 19, pp. 4445–4459, 2018.
- [4] O. Caytan, L. Bogaert, H. Li, J. Van Kerrebrouck, S. Lemey, S. Agneessens, J. Bauwelinck, P. Demeester, G. Torfs, D. Vande Ginste, and H. Rogier, “Compact and Wideband Transmit Opto-Antenna for Radio Frequency over Fiber,” *Opt. Express*, vol. 27, no. 6, pp. 8395–8413, 2019.
- [5] Q. Van den Brande, S. Lemey, S. Cuyvers, S. Poelman, L. De Brabander, O. Caytan, L. Bogaert, I. L. D. Paula, S. Verstuyft, A. C. F. Reniers, B. Smolders, B. Kuyken, D. Vande Ginste, and H. Rogier, “A Hybrid Integration Strategy for Compact, Broadband, and Highly Efficient Millimeter-Wave On-Chip Antennas,” *IEEE Antennas Wirel. Propag. Lett.*, vol. 18, pp. 2424–2428, Nov 2019.
- [6] G. Torfs, H. Li, S. Agneessens, J. Bauwelinck, L. Breyne, O. Caytan, W. Joseph, S. Lemey, H. Rogier, A. Thielens, D. Vande Ginste, J. Van Kerrebrouck, G. Vermeeren, X. Yin, and P. Demeester, “ATTO: Wireless networking at fiber speed,” *J. Light. Technol.*, vol. 36, pp. 1468–1477, April 2018.
- [7] P. Liu, L. Chang, Y. Li, Z. Zhang, S. Wang, and Z. Feng, “A millimeter-wave micromachined air-filled slot antenna fed by patch,” *IEEE T. Comp. Pack. Man.*, vol. 7, pp. 1683–1690, Oct 2017.
- [8] V. K. Singh, “Ka-band micromachined microstrip patch antenna,” *IET Microw. Antenna P.*, vol. 4, pp. 316–323, March 2010.
- [9] Y. Song, K. Kang, Y. Tian, Y. Wu, Z. Li, Y. Guo, Y. Ban, J. Liu, X. Tang, H. Liu, and J. Yang, “A hybrid integrated high-gain antenna with an on-chip radiator backed by off-chip ground for SoC applications,” *IEEE T. Comp. Pack. Man.*, vol. 7, pp. 114–122, Jan 2017.